Assessing the contribution of open crop straw burning to ground-level ozone and associated health impacts in China and the effectiveness of straw burning bans.

HUANG, L., ZHU, Y., LIU, H., WANG, Y., ALLEN, D.T., OOI, M.C.G., MANOMAIPHIBOON, K., LATIF, M.T., CHAN, A. and LI, L.

2023

Full length article

Assessing the contribution of open crop straw burning to ground-level ozone and associated health impacts in China and the effectiveness of straw burning bans

Ling Huang [a,b], Yonghui Zhu [a,b], Hanqing Liu [a,b], Yangjun Wang [a,b], David T. Allen [c], Maggie Chel Gee Ooi [d], Kasemsan Manomaiphiboon [e], Mohd Talib Latif [f], Andy Chan [g], Li Li [a,b,*]

[a] School of Environmental and Chemical Engineering, Shanghai University, Shanghai 200444, China
[b] Key Laboratory of Organic Compound Pollution Control Engineering (MOE), Shanghai University, Shanghai, China
[c] Center for Energy and Environmental Resources, University of Texas at Austin, 10100 Burnet Road, Austin, TX 78758, United States
[d] Institute of Climate Change (IPI), Universiti Kebangsaan Malaysia, 43600 Bangi, Selangor, Malaysia
[e] The Joint Graduate School of Energy and Environment, King Mongkut's University of Technology Thonburi, Bangkok 10140, Thailand
[f] Department of Earth Sciences and Environment, Faculty of Science and Technology, Universiti Kebangsaan Malaysia, 43600 Bangi, Selangor, Malaysia
[g] Department of Civil Engineering, University of Nottingham Malaysia, Semenyih 43500, Selangor, Malaysia

ARTICLE INFO

ABSTRACT

In recent years, ozone pollution in China has been shown to increase in frequency and persistence despite the concentrations of fine particulate matter ($PM_{2.5}$) decreasing steadily. Open crop straw burning (OCSB) activities are extensive in China and emit large amounts of trace gases during a short period that could lead to elevated ozone concentrations. This study addresses the impacts of OCSB emissions on ground-level ozone concentration and the associated health impact in China. Total VOCs and NOx emissions from OCSB in 2018 were 798.8 Gg and 80.6 Gg, respectively, with high emissions in Northeast China (31.7%) and North China (23.7%). Based on simulations conducted for 2018, OCSB emissions are estimated to contribute up to 0.95 μg/m^3 increase in annual averaged maximum daily 8-hour (MDA8) ozone and up to 1.35 μg/m^3 for the ozone season average. The significant impact of OCSB emissions on ozone is mainly characterized by localized and episodic (e.g., daily) changes in ozone concentration, up to 20 μg/m^3 in North China and Yangtze River Delta region and even more in Northeast China during the burning season. With the implementation of straw burning bans, VOCs and NOx emissions from OCSB dropped substantially by 46.9%, particularly over YRD (76%) and North China (60%). Consequently, reduced OCSB emissions result in an overall decrease in annual averaged MDA8 ozone, and reductions in monthly MDA8 ozone could be over 10 μg/m^3 in North China. The number of avoided premature death due to reduced OCSB emissions (considering both $PM_{2.5}$ and ozone) is estimated to be 6120 (95% Confidence Interval: 5320–6800), with most health benefits gained over east and central China. Our results illustrate the effectiveness of straw burning bans in reducing ozone concentrations at annual and national scales and the substantial ozone impacts from OCSB events at localized and episodic scales.

1. Introduction

Open biomass burning (OBB) could emit large amounts of trace gases and particulate matter during a short period, thereby exhibiting substantial impacts on air quality and public health at local and regional scales (Zha et al., 2013; Zhou et al., 2017; Zong et al., 2016). Emissions of primary aerosols directly result in elevated concentrations of fine particulate matter ($PM_{2.5}$). In contrast, emissions of gaseous species (e.

g., volatile organic compounds, VOCs) lead to the formation of secondary organic aerosols and ground-level ozone (O_3). The impacts of OBB on $PM_{2.5}$ concentration over different regions have been evaluated in many studies (Bossioli et al., 2016; Cheng et al., 2014; Huang et al., 2021; Wilkins et al., 2018; Yang et al., 2020; Zhou et al., 2018). Being an important type of biomass burning, open crop straw burning (OCSB) is a common management practice in China, especially during the harvesting, post-harvest or pre-planting periods. According to Hong et al.

(2016), the crop straw resources in China rank first in the world, accounting for 20% of global production. Numerous studies have demonstrated the important contribution of OCSB to atmospheric PM$_{2.5}$ in China. For instance, Cheng et al. (2014) showed that OBB contributed 37% of the observed PM$_{2.5}$ concentrations in the Yangtze River Delta (YRD) region of China. Zhou et al. (2018) investigated an intense biomass burning event in the North China Plain (NCP) and found that the contribution of OCSB to PM$_{2.5}$ concentration reached 19% in China. During a harvest season (November 2015) in Northeast China, OCSB contributed more than 50% to PM$_{2.5}$ concentration (Yang et al., 2020). To mitigate the PM$_{2.5}$ pollution in China, prohibition on OCSB activities (referred to as "straw burning bans") was proposed by the Chinese government, among many other control policies (Sun et al., 2019; Yang et al., 2020). According to our previous study (Huang et al., 2021), the national total PM$_{2.5}$ emissions from OCSB reduced by 46.9% from 2013 to 2018, and annual averaged PM$_{2.5}$ concentrations show widespread reductions over China with maximum decrease exceeding 2.0 μg/m^3 in East China.

On the other hand, observed ozone concentrations in key regions of China have shown a generally increasing trend from 2013 to 2018 (Fan et al., 2020), and the frequency and persistence of ozone pollution episodes are rising (Gong & Liao, 2019; Gong et al., 2020). Elevated ozone concentration negatively impacts human health, vegetation, and ecosystem production (Fleming et al., 2018; Mills et al., 2018; Xu et al., 2020). Consequently, ozone is listed as a co-control air pollutant along with PM$_{2.5}$ in China in the 14th Five-Year Plan for National Economic and Social Development of the People's Republic of China and the Vision for 2035 (http://www.gov.cn/xinwen/2021-03/13/content_5592681. htm, accessed on August 15th, 2022). Nevertheless, the control of ozone is much more complicated due to the nonlinearity of ozone chemistry to its precursors, namely nitrogen oxides (NOx) and VOCs, both of which are emitted simultaneously from burning activities. So far, only a limited number of studies have addressed the impact of biomass burning on local or regional ozone formation (Lee et al., 2019; Tang et al., 2013; Zhu et al., 2016). For example, Tang et al. (2013) found that agricultural straw burning in June increased ozone concentrations by 27%–39% in the YRD region. Most existing studies are either limited to certain areas or focused on a certain period of the burning episode. A multi-regional and year-long study of the impacts of OCSB on ground-level ozone concentration is needed for a comprehensive evaluation in China. Whether implementing the straw burning bans has also effectively reduced surface ozone concentration needs to be addressed.

As a follow-up to our previous study (Huang et al. 2021), the present work aims to address the impacts of OCSB on surface ozone concentration and public health in China and further evaluate the effectiveness of straw burning bans based on a typical modeling approach. Three objectives are to be achieved by this work. Firstly, the ozone contribution from OCSB emissions is quantified over different regions and seasons. Secondly, the effectiveness of straw burning bans in reducing ozone concentration is assessed. Lastly, the impacts on human health associated with ozone exposure under different scenarios are quantified. This work represents the first comprehensive modeling study evaluating the effects of OCSB emissions on ground-level ozone concentrations in China. Findings from this study shall provide useful information on future ozone control policies regarding open biomass burning.

2. Methods

2.1. VOCs and NOx emissions from open biomass burning

Ground-level ozone is formed via complicated photochemical reactions involving VOCs and NOx, both of which are emitted from burning activities, although their relative abundance differs by the burning materials. The widely-used Fire INventory from NCAR version 1.5 (FINNv1.5) (Wiedinmyer et al., 2011; https://www.acom.ucar. edu/Data/fire/) was adopted in this study to analyze the VOCs and

NOx emissions associated with different burning types. Based on satellite fire detection, FINN combines land cover data, emission factors, and fuel loadings to calculate emissions of various air pollutants from burning events in a bottom-up fashion (Wiedinmyer et al., 2006) with a high temporal (daily) and spatial resolution (~1km) (Wiedinmyer et al., 2011). The burning types in FINN are classified based on the MODIS land cover type and are further grouped into four types – forest, grassland, shrub, and cropland – for analyzing VOCs and NOx emissions.

2.2. Model configurations

To quantify the impacts of OCSB on ground-level ozone concentrations, the Weather Research Forecasting (WRF) model for meteorology simulation, followed by the Comprehensive Air Quality Model with Extensions (CAMx) for air quality simulation, is utilized in this work. The model configuration and input data can be found in our previous study (Huang et al. 2021) and briefly summarized here. The National Centers for Environment Prediction/Final Operational Global Analysis (NCEP/FNL) data is used to drive the WRF simulation. The gaseous and aerosol modules used in CAMx include the CB05 chemical mechanism (Yarwood et al., 2010) and the CF module. The aqueous-phase chemistry is based on the updated mechanism of the Regional Acid Deposition Model (RADM)(Chang et al., 1987). Simulations were conducted with a horizontal resolution of 36 km covering entire China and 23 vertical layers up to 50 hPa. Anthropogenic emissions for China are based on the Multi-resolution Emission Inventory of China for 2017 (MEIC, http://www.meicmodel.org, accessed on December 1st, 2021) developed by Tsinghua University. Emissions outside China are based on the European Commission's Emissions Database for Global Atmospheric Research (EDGAR, http://edgar.jrc.ec.europa.eu/index.php, accessed on December 1st, 2021) for 2010. Biogenic emissions are calculated by an updated version of the Model of Emissions of Gases and Aerosols from Nature (MEGAN, version 3.0, http://aqrp.ceer.utexas.edu/projects.cfm, accessed on November 10th, 2021). Open biomass burning emissions are based on FINN with MOZART speciation and converted to CAMx CB05 model species.

Annual simulations were conducted for 2018 with different OCSB emissions while keeping other model inputs and configurations unchanged (Table 1). In the base scenario, the FINN OCSB emissions for 2018 were used. In a second scenario, OCSB emissions were excluded, and the simulated ozone difference from the base scenario represents the contribution of OCSB emissions to ozone concentrations. In a third scenario, the OCSB emissions for 2018 in the base scenario were replaced by emissions from 2013. According to our previous study (Huang et al. 2021), 2013 was considered the beginning year for vigorously implementing the straw-burning bans. The changes in OCSB emissions between 2013 and 2018 reflect the control policy's effectiveness. The differences in simulated ozone concentration between the base and third scenarios were used to evaluate the effects of straw burning bans on ozone concentrations. Simulated meteorological variables such as temperature, wind speed, and relative humidity were verified in our previous work (Huang et al. 2021). The model performance of the base case ozone simulation was evaluated against the observations at 74 monitoring sites across China (Fig. 1) with commonly used metrics, including the Pearson correlation coefficient (R), mean bias (MB), normalized mean bias (NMB), root mean square error

Table 1
Emission configurations of different scenarios.

Scenario	Emissions besides OCSB	OCSB emissions
Scenario 1 (base)	MEIC 2017 + EDGAR 2010 + MEGAN + FINN 2018 for vegetation types except croplands	FINN 2018
Scenario 2		–
Scenario 3		FINN 2013
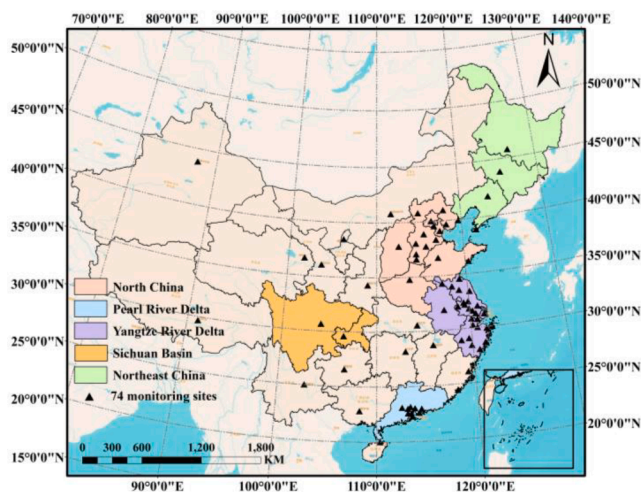
Fig. 1. Modeling domain with selected key regions.

(RMSE), and normalized mean error (NME) (see definitions in Table S1).

Five key regions were selected for further analysis of the impacts of biomass burning on ground-level ozone, including North China (including Beijing, Tianjin, province of Hebei, Shandong, Shanxi, and Henan), Yangtze River Delta (YRD) (Shanghai, province of Jiangsu, Anhui, and Zhejiang), Sichuan Basin (Chongqing, Sichuan province), Northeast China (province of Heilongjiang, Jilin, Liaoning) and Pearl River Delta and surrounding (i.e., Guangdong). These regions either have extensive burning activities (e.g., Northeast China) or suffer from elevated ozone concentration (e.g., YRD, Sichuan Basin) or both (North China) (Chen et al., 2017; Liu and Wang, 2020; Lu et al., 2019; Zhu et al., 2016).

2.3. Evaluation of health impacts associated with ozone exposure

According to existing epidemiological studies, chronic ozone exposure is mainly associated with respiratory and cardiovascular diseases (Jerrett et al., 2009; Turner et al., 2016). A commonly used method for studying the ozone exposure–response relationship is the epidemiological research approach, which quantifies the correlation between the health status of the population and the concentration of air pollutants through epidemiological surveys. In this study, the number of premature deaths due to cardiovascular disease (CVD) and respiratory disease (RD) attributable to ozone exposure is used to represent the health impact of ground-level ozone, which is calculated using Eq. (1)-(2), following many existing studies (e.g., Malley et al., 2017; Seltzer et al., 2018; Wang et al., 2020):

$$RR(C) = \begin{cases} e^{\beta(C-C_0)}, C > C_0 \\ 1, C \leq C_0 \end{cases} \tag{1}$$

$$H = \sum B \times P \times \frac{RR-1}{RR} \tag{2}$$

where RR is the relative risk, i.e. the probability of a particular health endpoint associated with a 10 ppb increase in ozone concentration (Cairncross et al., 2007; Liu et al., 2018); β is the observation-based concentration response factor, i.e., the slope of the log-linear relationship between exposure concentration and mortality; C represents the value of a specific ozone indicator, and C_0 is the threshold below which there is no adverse effect. In Eq. (3), H is the estimated number of premature deaths; B is the provincial incidence rate of a specific disease, obtained from the online GBD database (https://vizhub.healthdata.org/gbd-compare/, accessed on December 1st, 2021); P is the exposed population for each province in China, which is obtained from the 2019 statistical yearbook. We used the annual mean daily 8-hour maximum ozone concentration (AMDA8) as the ozone indicator and adopted a

threshold of 26.7 ppb following Turner et al. (2016).

3. Results and discussions

3.1. OCSB emissions of ozone precursors

According to FINN estimates, the annual total VOCs and NO*x* emissions from OCSB activities for year 2018 in China are estimated to be 798.8 Gg and 80.6 Gg, respectively. In terms of the emitted VOCs species, oxygenated-VOCs (OVOCs) represents the dominant group (70%), followed by aromatics (15%) and alkenes (12%) (Table S2). The high VOCs/NO*x* emission ratio range (~10) for OCSB suggests a NO*x*-limited environment within the fire plume, yet the impacts on ozone formation could be different, especially when mixed with different background emissions downwind the fire plume. Spatially, OCSB activities occur frequently in Northeast China, North China, and northern YRD, which are the major agricultural regions in China (Fig. 2). With respect to the seasonal variations, OCSB emissions show huge peaks in March and April in Northeast China, whereas in North China and YRD, OCSB emissions are more evenly distributed from February to November. Although the annual total VOCs and NO*x* emissions due to OCSB only account for 3.4% and 0.4% compared to the anthropogenic emissions (Table S3), the impact of OCSB emissions should not be ignored given the episodic and localized feature of the burning activities.

3.2. Impact of OCSB emissions on ground-level ozone concentrations

3.2.1. Base case evaluation

Fig. 3 shows the spatial distribution of the simulated seasonal daily maximum 8-hour average (MDA8) ozone concentration in 2018 against observations. Values of MB, RMSE, NMB, NME, and R of daily MDA8 ozone concentration by season and region are provided in Table S4. Results for other pollutants can be found in Huang et al. (2021). In general, the model well captures the spatial distribution and seasonal variations of the observed ozone concentration. The model tends to overestimate ozone concentrations for all regions except in Northeast China. The observed AMDA8 concentration averaged over 74 monitoring sites is 77.0 ppb, contrasted to the simulated value of 83.8 ppb. Sichuan Basin shows the highest overestimation, also found in other studies (Hu et al., 2016). In terms of the seasonal results, NMB is all within 15%, and summer shows the highest R value. According to Eq.1, premature mortality increases exponentially with the ozone concentration, with a steeper slope near the threshold and a milder slope at higher ozone concentrations. This indicates the same relative bias in the simulated ozone concentration would cause more deviation at low ozone concentration near the threshold. For those 74 monitoring sites, we estimated an overestimated premature mortality by 10.5% when simulated ozone concentrations were used.

3.2.2. Impact of OCSB emissions on ground-level ozone

As shown by Fig. 4, OCSB emissions lead to a widespread increase in annually averaged ozone concentrations and during ozone season (April-October) across China. Regions with high ozone impacts include North China, Northeast China, and northern YRD, which aligns with the high OCSB emission regions (Fig. 2). For AMDA8, the maximum increase due to OCSB emissions reaches 0.95 μg/m³ in North China; for ozone season averages, OCSB emissions contribute up to 1.35 μg/m³ of ozone enhancement over North China. Since OCSB emissions are characterized as intermittent and point emissions, it is reasonable to look at the impacts on daily ozone changes and grid-cell levels. As illustrated by Fig. 5, both positive and negative impacts were observed in terms of daily MDA8 ozone change at the grid cell level and the magnitudes and temporal variations closely follow that of OCSB emissions. For example, in Northeast China, while most grid cells showed increased ozone concentration due to OCSB emissions in March (up to 70 μg/m³), a few grid cells showed decreased ozone concentration with the inclusion of OCSB
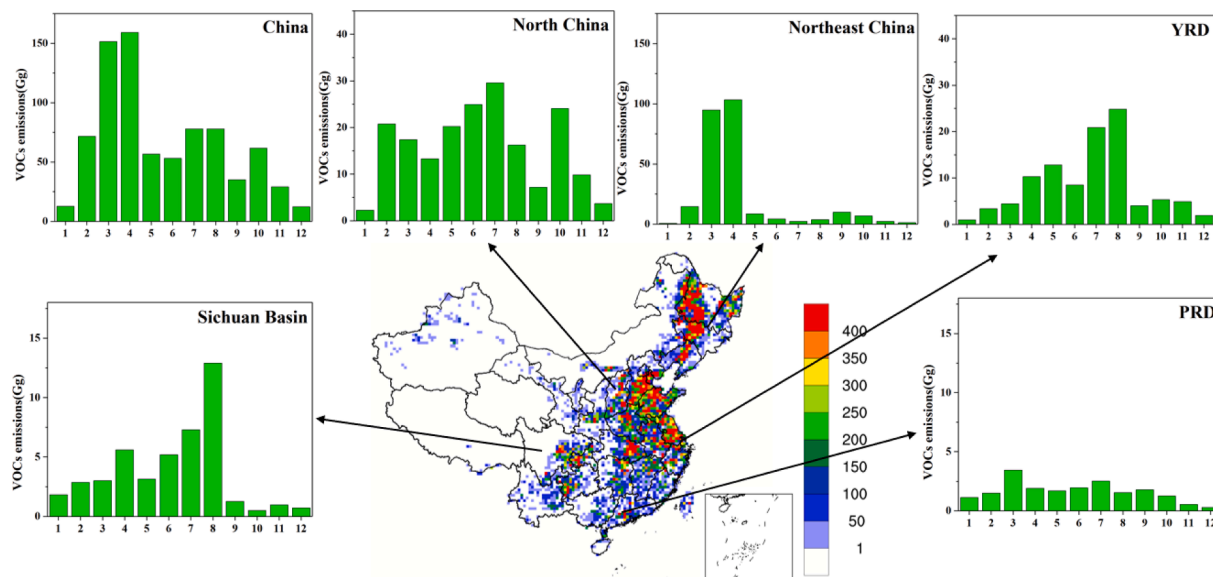
Fig. 2. Spatial distribution of annual VOCs emissions from OCSB ($\times 10^{-3}$ Gg) with monthly variations for selected regions (Corresponding plots for NOx are presented in Fig. S1).
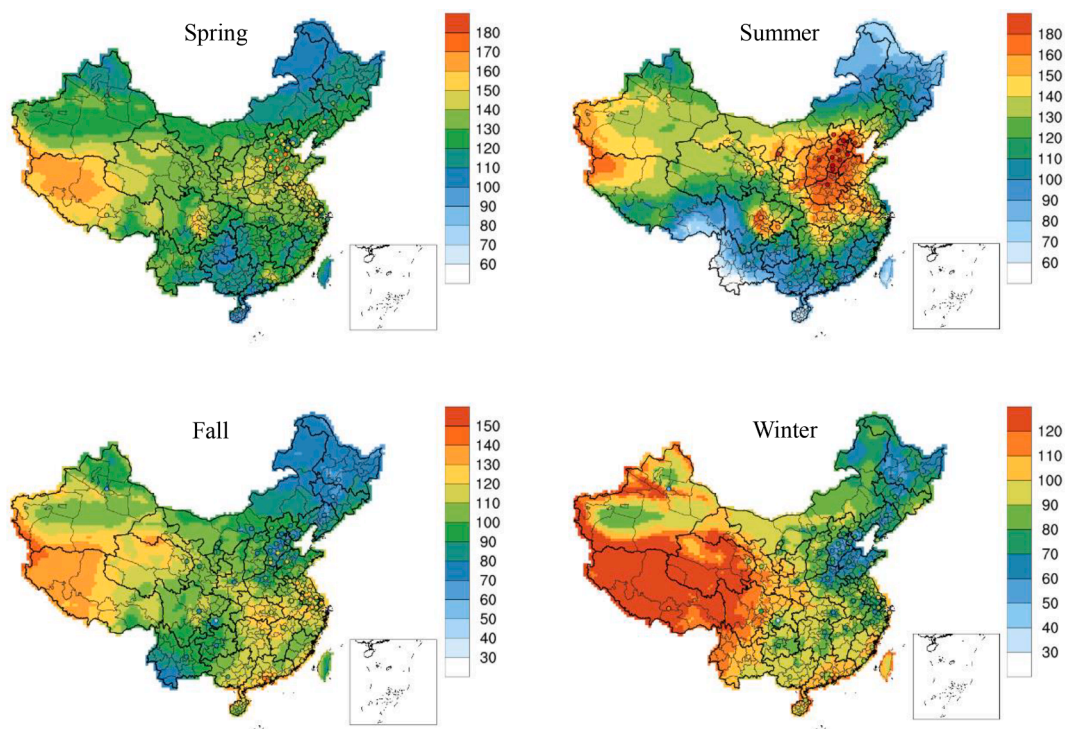
Fig. 3. Spatial distribution of simulated versus observed seasonal MDA8 ozone concentrations (µg/m^3) in 2018 (observed values shown by dots).

emissions. In North China and YRD, OCSB emissions exhibit substantial impacts from April to October, with more ozone increase (by as much as 20 µg/m^3) than ozone reduction. The effects of OCSB emissions on daily ozone changes over the Sichuan Basin, PRD, and surrounding regions are within +/-10 µg/m^3. The different ozone response to OCSB activities in localized areas reflects the non-linearity of the ozone formation chemistry, where reduced NOx emissions do not always lead to ozone reduction, usually under a VOC-limited regime. The changes in ozone concentrations are determined by the local ozone formation regime as well as influenced by the transport of NOx and VOC emissions from upwind crop burning activities. Further studies are needed to investigate

the underlying mechanism of the ozone response to representative burning events over different regions and under different meteorological conditions.

We further evaluate the impact of OCSB emissions on the cumulative number of ozone exceedances days (defined as days with MDA8 ozone concentration higher than 160 µg/m^3 according to China's Ambient Air Quality Standards) for cities in the selected five regions. The ozone exceedances days range from a total of 323 days in PRD and surrounding (~36 days per city) to as many as 4544 days in North China (~65 days per city) in 2018 (Table 2 and Table S5). For all regions except PRD, ozone exceedance days mainly occur in April-August, and June has the
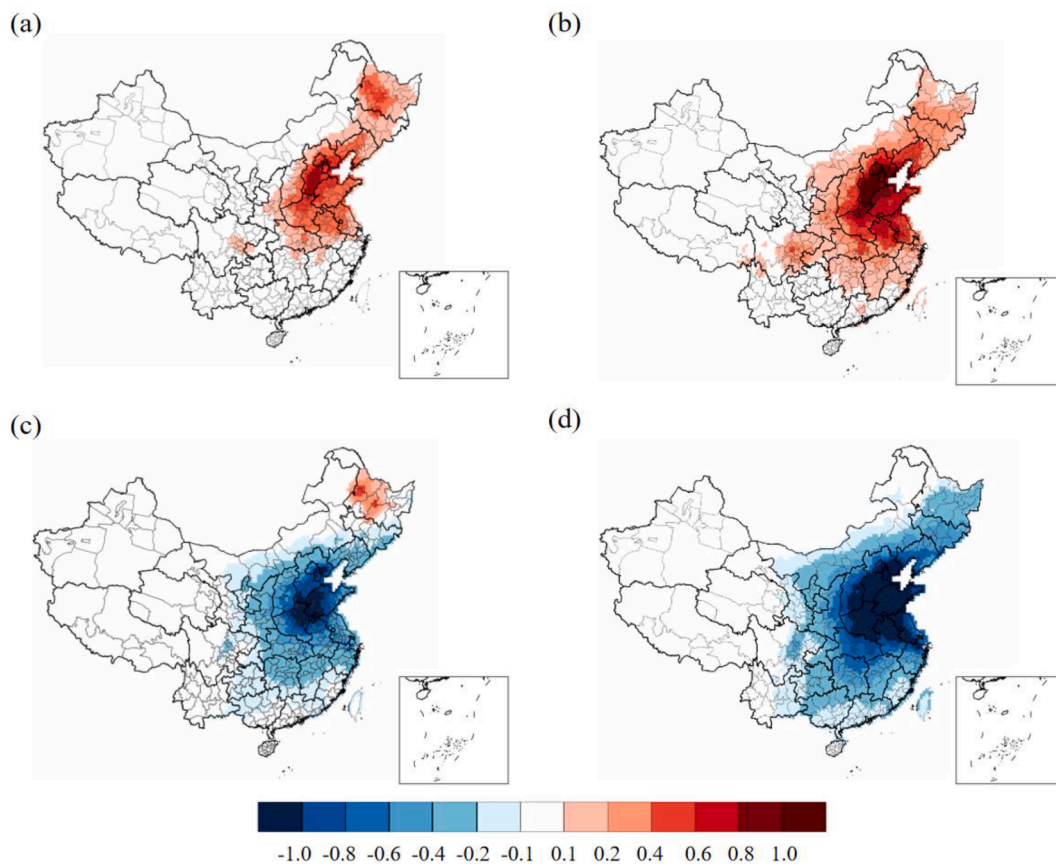
Fig. 4. Spatial distribution of changes in AMDA8 ozone and MDA8 ozone during ozone season (April-October) due to OCSB emissions (a, b) and straw burning bans (c, d) Unit: μg/m³.
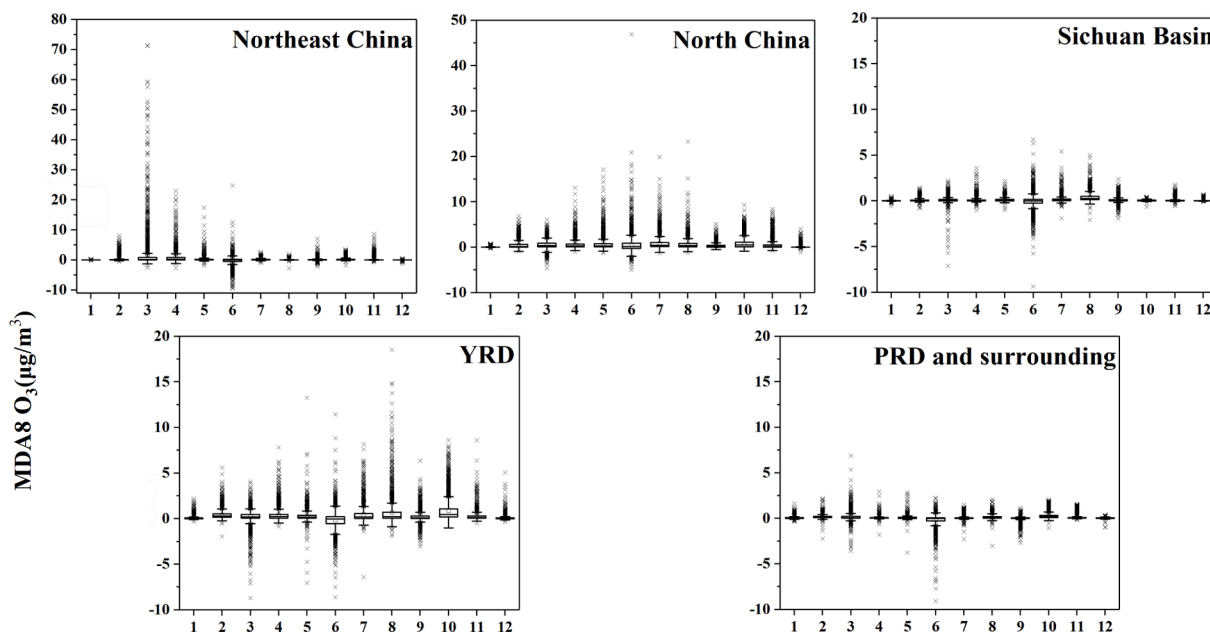
Fig. 5. Changes of monthly averaged MDA8 ozone concentration (μg/m³) due to OCSB emissions.

most ozone exceedance days (except Sichuan Basin) (Fig. S2). We applied the method of relative response factor (RRF, calculated as the ratio of simulated ozone concentration from Scenario 2 to simulated ozone concentration from base scenario) to obtain the adjusted ozone concentration when OCSB emissions are removed. Results show that

OCSB emissions increase the number of ozone exceedances days by 2 to 106 days. North China shows the most significant increase in ozone exceedance days (+106 days) due to the OCSB emissions. The maximum increase in ozone exceedance days reaches four days at the city level. In YRD and Northeast China, ozone exceedances increased by 33 days and

Table 2
Changes in the number of ozone exceedances days for selected regions in 2018.

Region (No. of cities)	Number of ozone exceedances days	Δ ozone exceedances days due to OCSB emissions	Δ ozone exceedances days due to straw burning bans
North China (70)	4,544	+106	−138
YRD (56)	2,447	+33	−103
Sichuan Basin (22)	479	+5	−13
Northeast China (36)	746	+18	−31
PRD (9)	323	+2	−2

18 days due to OCSB emissions, whereas changes in Sichuan Basin and PRD are relatively small given that the OCSB emissions are comparatively lower in these two regions.

3.2.3. Impact of the straw burning bans

Consistent with the trends of PM$_{2.5}$ emissions described in our previous study (Huang et al., 2021), the total VOC emissions from OCSB exhibit an overall downward trend from 2010 to 2018, with two distinct peaks in 2013 and 2017 (Fig. 6). The first peak in 2013 was mainly contributed by emissions from North China (32%) and YRD (29%), exhibiting a sharp decreasing trend after 2013. The 2017 peak is predominantly contributed by Northeast China, which showed a continuous increase in OCSB emissions during 2010–2017, followed by a drastic drop in 2018. Compared with 2013, VOCs and NOx emissions from OCSB in 2018 decreased by 703 Gg and 71 Gg (both decreased by 47%), with a maximum reduction in June by 87%. YRD (by 76%) and North China (by 60%) show a significant decline in OCSB emissions, whereas Northeast China was the only region with increased OCSB emissions in 2018, especially in February-April (Fig. S3). The implementation of straw burning bans in Northeast China lagged relatively behind other regions (most policies were announced in 2017). During 2013–2017, Northeast China witnessed a continuous increase in OCSB activities, with a relative increase of VOC emissions by 235% in 2017 compared to 2013. Although a sharp reduction in OCSB emissions was observed in 2018 (reduced by 66% compared to 2017), it did not entirely offset the increased emissions from 2013 to 2017. Based on the existing results, the impacts on ozone concentration are proportional to the magnitude of OCSB emissions. Thus it is expected the impacts of OCSB emissions on ozone concentration would be the most significant in 2017, especially during March-April.
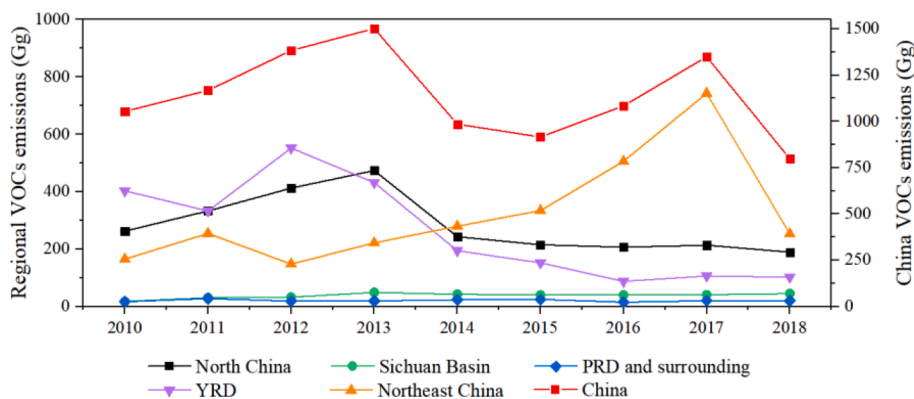
To assess the impact of straw burning bans on ground-level ozone concentration, we replaced 2018 OCSB emissions in the base scenario with 2013 OCSB emissions (i.e., Scenario 3) while keeping all the other emissions and model configurations unchanged. Fig. 6c-d shows the spatial distribution of the annual average and ozone season averaged change of MDA8 ozone before and after implementing straw burning bans. Except for Northeast China where OCSB emissions increased in 2018 compared to 2013, AMDA8 ozone concentrations generally decreased, with North China and YRD showing the most significant declines. Regional averaged ozone decreased by 0.69 μg/m^3 and 0.49 μg/m^3 for North China and YRD, with the largest localized decrease up to 1.3 μg/m^3. Regarding the ozone season change (Fig. 4d), the maximum MDA8 ozone concentration decreased by up to 1.30 μg/m^3 in North China and up to 0.94 μg/m^3 in YRD.

Fig. 7 shows the changes in monthly average MDA8 ozone due to the implementation of straw burning bans. North China and YRD show overall reductions in monthly average MDA8 ozone, with the most reductions in June, which is also the month with the highest number of ozone exceedances days. Regional averaged MDA8 ozone decreased by 5.4 μg/m^3 and 2.8 μg/m^3 in June in North China and YRD, with a maximum decrease exceeding 10 μg/m^3 at specific locations. This large decrease corresponds to the significant reduction of OCSB emissions in June (86% in North China and 95% in YRD). Northeast China exhibits increases in monthly MDA8 ozone concentrations during the burning seasons (March-April), with an average increase of 1.6 μg/m^3 in March and a maximum increase of 7.2 μg/m^3 due to increased OCSB emissions. The implementation of straw burning bans reduces the cumulative number of ozone exceedances days by 2 to 138 days for different regions (Table 2). Again, North China shows the largest decrease in ozone exceedance days by 138 days, followed by YRD (103 days) and Northeast China (31 days).

3.3. Health impact associated with OCSB

Based on the method described in Section 2.3, the number of premature deaths due to cardiovascular disease (CVD) and respiratory disease (RD) under different scenarios was estimated (Table S6). Under the base scenario, the national total number of premature deaths due to ozone exposure in 2018 was estimated to be 288,000 (95% Confidence Interval (CI): 164,000–401,000), which is relatively consistent with the values estimated by previous studies (e.g., Wang et al., 2020). As calculated in our previous study, this value is around 70% lower than that due to PM$_{2.5}$ exposure in 2018. RD and CVD account for 61% and 39% of the total premature deaths, respectively. The spatial distribution of premature mortality due to ozone exposure concentrated over North China which has both high population density and high ozone concentrations (Fig. S4). The top five provinces that have the highest premature mortality due to ozone exposure include Shandong (23,980, 95% CI:13,640–33,390), Sichuan (23,650, 95% CI:13,510–32,820), Henan

Fig. 6. Emissions of VOCs from OCSB in China by region from 2010 to 2018.
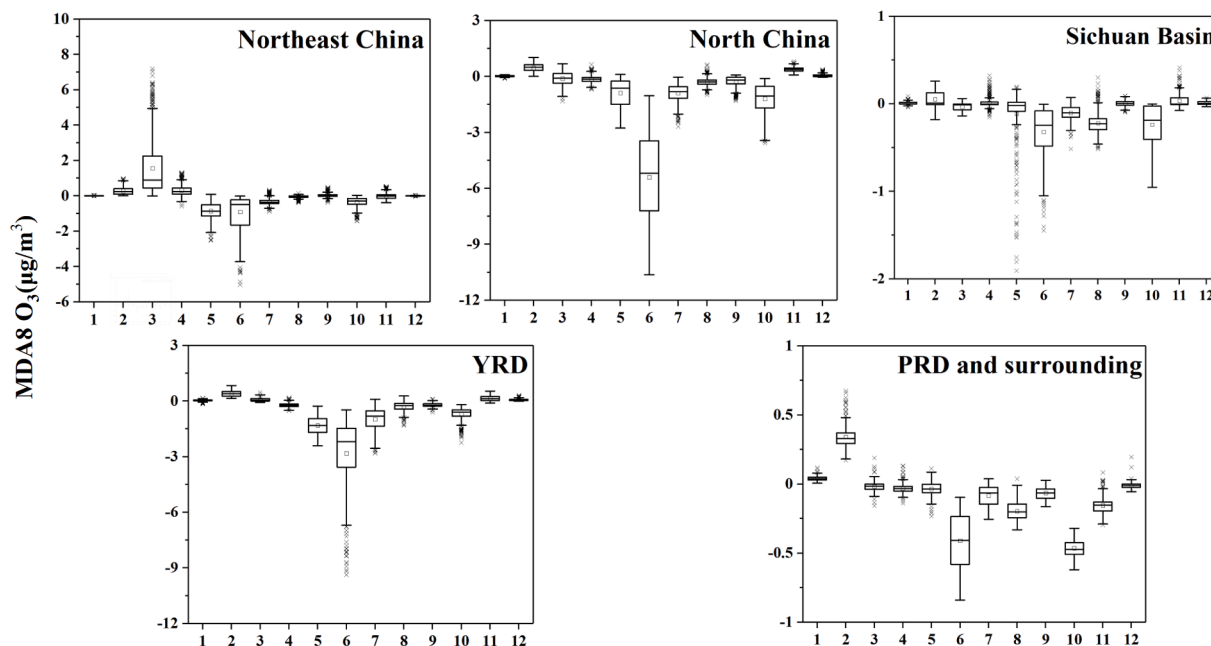
Fig. 7. Change of monthly MDA8 O₃ due to OCSB emission changes between 2013 and 2018 by region and month.

(22,050, 95% CI:12,580–30,610), Jiangsu (19,030, 95% CI:10,830–26,510), and Guangdong (17,420, 95% CI: 9900–24,310).

The total number of premature deaths due to ozone exposure attributable to OCSB emissions in 2018 was estimated to be 1550 (95% CI: 880–2010), accounting for 0.54% of ozone-related premature mortality. As expected, regions with evident health impacts are regions with high OCSB emissions and high populations (Fig. 8). The five provinces that have the highest OCSB related health impacts are Shandong (230, 95% CI: 120–300), Hebei(220, 95% CI: 140–310), Henan (180, 95% CI: 100–240), Jiangsu (120, 95% CI: 70–160), and Anhui (110, 95% CI:

60–140). If OCSB emissions were kept at 2013 levels, the total number of premature deaths associated with ozone exposure would increase by 1870 (95% CI: 1070–2550) (a relative increase of 0.65%). Shandong (360, 95% CI: 210–490), Henan (280, 95% CI: 170–390), Hebei (270, 95% CI: 160–260), Jiangsu (170, 95% CI: 100–230), and Anhui (140, 95% CI: 90–200) are the top five provinces that have the highest number of avoided premature mortality as the result of straw burning bans. When summed with our previous results of premature mortality associated with PM2.5 exposure (Huang et al. 2021), the total number of premature deaths attributed to OCSB emissions (considering both ozone
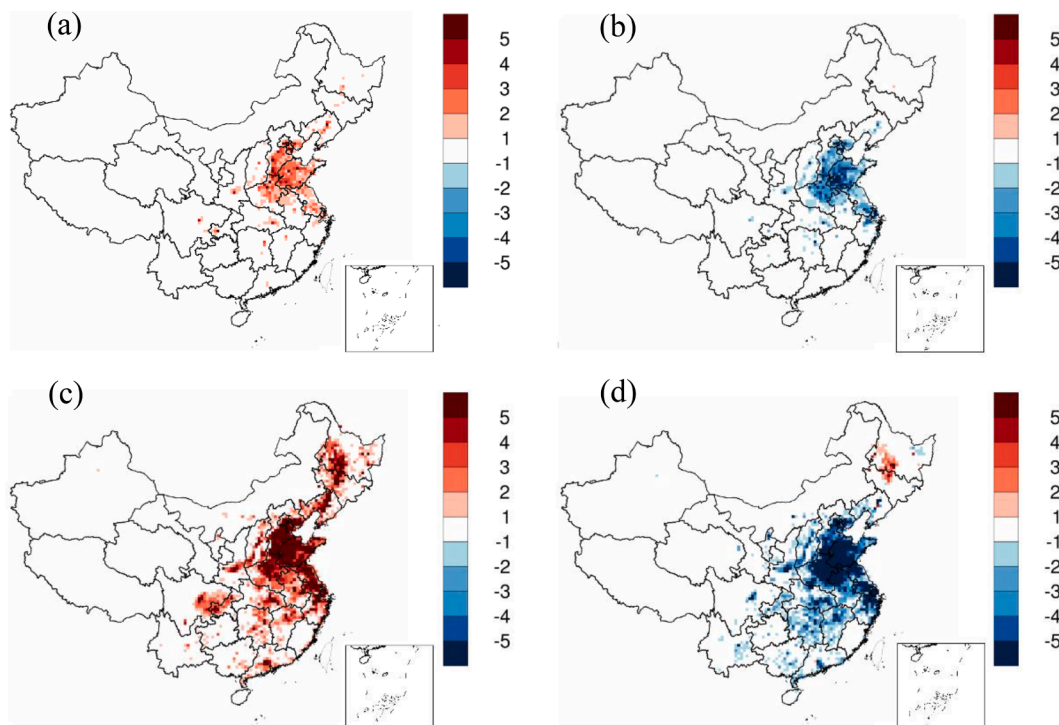
Fig. 8. Spatial distribution of premature mortality associated with ozone exposure (upper row) and associated with both PM2.5 and ozone exposure (bottom row) due to OCSB emissions (left) and straw burning bans (right) (No data for Taiwan, Hong Kong, and Macau) Unit: person/grid.

and PM$_{2.5}$ exposure) in 2018 was 6290 (95% CI: 5620–6750). The implementation of the straw burning bans reduced the total number of premature death by 6120 (95% CI: 5320–6800), suggesting substantial health benefits of the control policy. The top five provinces that gained the most health benefits from the straw burning bans are Shandong (880, 95% CI: 730–1010), Henan (760, 95% CI: 650–870), and Anhui (590, 95% CI: 540–650).

4. Conclusions

Open crop straw burning (OCSB) represents an important source of VOCs and NOx emissions in China that could affect ground-level ozone formation. In 2018, the total annual VOCs and NOx emissions from OSCB activities were 798.8 Gg and 80.6 Gg, respectively, with high emissions located in North China, Northeast China, and northern YRD and distinct monthly variations across different regions. Our model simulation results show that OCSB emissions resulted in a widespread increase in annual average (up to 0.95 μg/m^3) and ozone season average (up to 1.35 μg/m^3) MDA8 in 2018, with North China exhibiting the strongest ozone impacts where the burning season coincides with the most severe ozone pollution month (i.e., June). OCSB emissions significantly impact daily and localized ozone concentrations, which could be up to 20 μg/m^3 in North China and YRD region and even more in Northeast China during the burning season.

In addition, we show that the implementation of straw burning bans substantially reduces the overall VOCs and NOx emissions from OCSB activities by 47% when comparing 2018 to 2013, although Northeast China is an exception. Regional averaged MDA8 ozone decreased by 5.4 μg/m^3 and 2.8 μg/m^3 in June in North China and YRD, with a maximum decrease exceeding 10 μg/m^3 at specific locations. Due to the straw burning bans, the cumulative number of ozone exceedance days was reduced by 4 to 138 days for selected regions. Based on a concentration–response function, the total number of premature deaths attributed to OCSB emissions (considering both PM$_{2.5}$ and ozone exposure) in 2018 was estimated to be 6290 (95% CI: 5620–6750), and the implementing the straw burning bans reduced the number of premature death by 6120 (95% CI: 5320–6800), suggesting substantial health benefits from the control policy.

CRediT authorship contribution statement

Ling Huang: Conceptualization, Formal analysis, Writing – original draft. **Yonghui Zhu:** Data curation, Formal analysis, Visualization. **Hanqing Liu:** . **Yangjun Wang:** Resources. **David T. Allen:** Writing – review & editing. **Maggie Chel Gee Ooi:** Writing – review & editing. **Kasemsan Manomaiphiboon:** Writing – review & editing. **Mohd Talib Latif:** Writing – review & editing. **Andy Chan:** Writing – review & editing. **Li Li:** Conceptualization, Supervision, Funding acquisition.

Declaration of Competing Interest

The authors declare that they have no known competing financial interests or personal relationships that could have appeared to influence the work reported in this paper.

Data availability

Data will be made available on request.

Acknowledgment

Appendix A. Supplementary material

Supplementary data to this article can be found online at https://doi.org/10.1016/j.envint.2022.107710.

References

Bossioli, E., Tombrou, M., Kalogiros, J., Allan, J., Bacak, A., Bezantakos, S., Biskos, G., Coe, H., Jones, B.T., Kouvarakis, G., Mihalopoulos, N., Percival, C.J., 2016. Atmospheric composition in the Eastern Mediterranean: Influence of biomass burning during summertime using the WRF-Chem model. Atmos. Environ. 132, 317–331.

Cairncross, E.K., John, J., Zunckel, M., 2007. A novel air pollution index based on the relative risk of daily mortality associated with short-term exposure to common air pollutants. Atmos. Environ. 41 (38), 8442–8454.

Chang, J., Brost, R., Isaksen, I., Madronich, S., Middleton, P., Stockwell, W., Walcek, C.J.o.G.R.A., 1987. A three-dimensional Eulerian acid deposition model. Phys. Concepts Formulation. 92 (D12), 14681–14700.

Chen, J., Li, C., Ristovski, Z., Milic, A., Gu, Y., Islam, M.S., Wang, S., Hao, J., Zhang, H., He, C., Guo, H., Fu, H., Miljevic, B., Morawska, L., Phong, T., Lam, Y.F., Pereira, G., Ding, A., Huang, X., Dumka, U.C., 2017. A review of biomass burning: emissions and impacts on air quality, health and climate in China. Sci. Total Environ. 579, 1000–1034.

Cheng, Z., Wang, S., Fu, X., Watson, J.G., Jiang, J., Fu, Q., Chen, C., Xu, B., Yu, J., Chow, J.C., Hao, J., 2014. Impact of biomass burning on haze pollution in the Yangtze River delta, China: a case study in summer 2011. Atmos. Chem. Phys. 14 (9), 4573–4585.

Fan, H., Zhao, C., Yang, Y., 2020. A comprehensive analysis of the spatio-temporal variation of urban air pollution in China during 2014–2018. Atmos. Environ. 220.

Fleming, Z.L., Doherty, R.M., von Schneidemesser, E., Malley, C.S., Cooper, O.R., Pinto, J.P., Colette, A., Xu, X., Simpson, D., Schultz, M.G., Lefohn, A.S., Hamad, S., Moolla, R., Solberg, S., Feng, Z., 2018. Tropospheric Ozone Assessment Report: Present-day ozone distribution and trends relevant to human health. Elementa-Sci. Anthropocene 6.

Gong, C., Liao, H., 2019. A typical weather pattern for ozone pollution events in North China. Atmos. Chem. Phys. 19 (22), 13725–13740.

Gong, C., Liao, H., Zhang, L., Yue, X., Dang, R., Yang, Y., 2020. Persistent ozone pollution episodes in North China exacerbated by regional transport. Environ. Pollut. 265, 115056.

Hong, J., Ren, L., Hong, J., Xu, C., 2016. Environmental impact assessment of corn straw utilization in China. J. Clean. Prod. 112, 1700–1708.

Hu, J., Chen, J., Ying, Q., Zhang, H., 2016. One-year simulation of ozone and particulate matter in China using WRF/CMAQ modeling system. Atmos. Chem. Phys. 16 (16), 10333–10350.

Huang, L., Zhu, Y., Wang, Q., Zhu, A., Liu, Z., Wang, Y., Allen, D.T., Li, L., 2021. Assessment of the effects of straw burning bans in China: emissions, air quality, and health impacts. Sci. Total Environ. 789.

Jerrett, M., Burnett, R.T., Pope II, C.A., Ito, K., Thurston, G., Krewski, D., Shi, Y., Calle, E., Thun, M., 2009. Long-term ozone exposure and mortality. N. Engl. J. Med. 360 (11), 1085–1095.

Lee, Y.C., Chan, K.L., Wenig, M.O., 2019. Springtime warming and biomass burning causing ozone episodes in South and Southwest China. Air Qual. Atmos. Health 12 (8), 919–931.

Liu, H., Liu, S., Xue, B., Lv, Z., Meng, Z., Yang, X., Xue, T., Yu, Q., He, K., 2018. Ground-level ozone pollution and its health impacts in China. Atmos. Environ. 173, 223–230.

Liu, Y., Wang, T., 2020. Worsening urban ozone pollution in China from 2013 to 2017-Part 1: the complex and varying roles of meteorology. Atmos. Chem. Phys. 20 (11), 6305–6321.

Lu, H., Lyu, X., Cheng, H., Ling, Z., Guo, H., 2019. Overview on the spatial-temporal characteristics of the ozone formation regime in China. Environ. Sci.-Processes Impacts 21 (6), 916–929.

Malley, C.S., Henze, D.K., Kuylenstierna, J.C.I., Vallack, H.W., Davila, Y., Anenberg, S.C., Turner, M.C., Ashmore, M.R., 2017. Updated global estimates of respiratory mortality in adults $>=$ 30 years of age attributable to long-term ozone exposure. Environ. Health Perspect. 125 (8).

Mills, G., Pleijel, H., Malley, C.S., Sinha, B., Cooper, O.R., Schultz, M.G., Neufeld, H.S., Simpson, D., Sharps, K., Feng, Z., Gerosa, G., Harmens, H., Kobayashi, K., Saxena, P., Paoletti, E., Sinha, V., Xu, X., 2018. Tropospheric Ozone Assessment Report: Present-day tropospheric ozone distribution and trends relevant to vegetation. Elementa-Sci. Anthropocene 6.

Seltzer, K.M., Shindell, D.T., Malley, C.S., 2018. Measurement-based assessment of health burdens from long-term ozone exposure in the United States, Europe, and China. Environ. Res. Lett. 13 (10).

Sun, D., Ge, Y., Zhou, Y., 2019. Punishing and rewarding: How do policy measures affect crop straw use by farmers? An empirical analysis of Jiangsu Province of China. Energy Policy 134.

Tang, H., Liu, G., Zhu, J., Han, Y., Kobayashi, K., 2013. Seasonal variations in surface ozone as influenced by Asian summer monsoon and biomass burning in agricultural fields of the northern Yangtze River Delta. Atmos. Res. 122, 67–76.

Turner, M.C., Jerrett, M., Pope III, C.A., Krewski, D., Gapstur, S.M., Diver, W.R., Beckerman, B.S., Marshall, J.D., Su, J., Crouse, D.L., Burnett, R.T., 2016. Long-term ozone exposure and mortality in a large prospective study. Am. J. Respir. Crit. Care Med. 193 (10), 1134–1142.

Wang, Y., Wild, O., Chen, X., Wu, Q., Gao, M., Chen, H., Qi, Y., Wang, Z., 2020. Health impacts of long-term ozone exposure in China over 2013–2017. Environ. Int. 144.

Wiedinmyer, C., Akagi, S.K., Yokelson, R.J., Emmons, L.K., Al-Saadi, J.A., Orlando, J.J., Soja, A.J., 2011. The Fire INventory from NCAR (FINN): a high resolution global model to estimate the emissions from open burning. Geosci. Model Dev. 4 (3), 625–641.

Wiedinmyer, C., Quayle, B., Geron, C., Belote, A., McKenzie, D., Zhang, X., O'Neill, S., Wynne, K.K., 2006. Estimating emissions from fires in North America for air quality modeling. Atmos. Environ. 40 (19), 3419–3432.

Wilkins, J.L., Pouliot, G., Foley, K., Appel, W., Pierce, T., 2018. The impact of US wildland fires on ozone and particulate matter: a comparison of measurements and CMAQ model predictions from 2008 to 2012. Int. J. Wildland Fire 27 (10), 684–698.

Xu, X., Lin, W., Xu, W., Jin, J., Wang, Y., Zhang, G., Zhang, X., Ma, Z., Dong, Y., Ma, Q., Yu, D., Li, Z., Wang, D., Zhao, H., 2020. Long-term changes of regional ozone in China: implications for human health and ecosystem impacts. Elementa-Sci. Anthropocene 8.

Yang, G., Zhao, H., Tong, D.Q., Xiu, A., Zhang, X., Gao, C., 2020. Impacts of post-harvest open biomass burning and burning ban policy on severe haze in the Northeastern China. Sci. Total Environ. 716.

Yarwood, G., Jung, J., Whitten, G.Z., Heo, G., Mellberg, J., Estes, M., 2010. Updates to the Carbon Bond mechanism for version 6 (CB6). In: 9th Annual CMAS Conference, Chapel Hill, NC.

Zha, S., Zhang, S., Cheng, T., Chen, J., Huang, G., Li, X., Wang, Q., 2013. Agricultural fires and their potential impacts on regional air quality over China. Aerosol Air Qual. Res. 13 (3), 992–1001.

Zhou, Y., Han, Z., Liu, R., Zhu, B., Li, J., Zhang, R., 2018. A modeling study of the impact of crop residue burning on PM2.5 concentration in beijing and tianjin during a severe autumn haze event. Aerosol Air Qual. Res. 18 (7), 1558–1572.

Zhou, Y., Xing, X., Lang, J., Chen, D., Cheng, S., Wei, L., Wei, X., Liu, C., 2017. A comprehensive biomass burning emission inventory with high spatial and temporal resolution in China. Atmos. Chem. Phys. 17 (4), 2839–2864.

Zhu, Y., Yang, L., Chen, J., Wang, X., Xue, L., Sui, X., Wen, L., Xu, C., Yao, L., Zhang, J., Shao, M., Lu, S., Wang, W., 2016. Characteristics of ambient volatile organic compounds and the influence of biomass burning at a rural site in Northern China during summer 2013. Atmos. Environ. 124, 156–165.

Zong, Z., Wang, X., Tian, C., Chen, Y., Qu, L., Ji, L., Zhi, G., Li, J., Zhang, G., 2016. Source apportionment of PM2.5 at a regional background site in North China using PMF linked with radiocarbon analysis: insight into the contribution of biomass burning. Atmos. Chem. Phys. 16 (17), 11249–11265.

Further reading

Carter, W.P., 2009. Updated maximum incremental reactivity scale and hydrocarbon bin reactivities for regulatory applications. California Air Resources Board Contract 339, 2009.

Guan, Y., Xiao, Y., Wang, F., Qiu, X., Zhang, N., 2021a. Health impacts attributable to ambient PM2.5 and ozone pollution in major Chinese cities at seasonal-level. J. Clean. Prod. 311.

Guan, Y., Xiao, Y., Wang, Y., Zhang, N., Chu, C., 2021b. Assessing the health impacts attributable to PM2.5 and ozone pollution in 338 Chinese cities from 2015 to 2020. Environ. Pollut. 287.

Li, A., Zhou, Q., Xu, Q., 2021a. Prospects for ozone pollution control in China: an epidemiological perspective. Environ. Pollut. 285.

Li, K., Jacob, D.J., Liao, H., Qiu, Y., Shen, L., Zhai, S., Bates, K.H., Sulprizio, M.P., Song, S., Lu, X., Zhang, Q., Zheng, B., Zhang, Y., Zhang, J., Lee, H.C., Kuk, S.K., 2021. Ozone pollution in the North China Plain spreading into the late-winter haze season. Proceedings of the National Academy of Sciences of the United States of America 118 (10).

Mehmood, K., Chang, S., Yu, S., Wang, L., Li, P., Li, Z., Liu, W., Rosenfeld, D., Seinfeld, J. H., 2018. Spatial and temporal distributions of air pollutant emissions from open crop straw and biomass burnings in China from 2002 to 2016. Environ. Chem. Lett. 16 (1), 301–309.

Streets, D.G., Yarber, K.F., Woo, J.H., Carmichael, G.R., 2003. Biomass burning in Asia: annual and seasonal estimates and atmospheric emissions. Global Biogeochem. Cycles 17 (4).

Zhou, Y., Zhang, Y., Zhao, B., Lang, J., Xia, X., Chen, D., Cheng, S., 2021. Estimating air pollutant emissions from crop residue open burning through a calculation of open burning proportion based on satellite-derived fire radiative energy. Environ. Pollut. 286.

Supplement of

Assessing the contribution of open crop straw burning to ground-level ozone and associated health impacts in China and the effectiveness of straw burning bans

Ling Huang, et al.

Correspondence to: Li Li (lily@shu.edu.cn)

Content

Table S1 Definition of model performance evaluation metrics used in in this study

No.	Statistics (abbreviation)	Definition	Note
1	Correlation coefficient (R)	$$\frac{\sum[(P_j - \bar{P}) \times (O_j - \bar{O})]}{\sqrt{\sum(P_j - \bar{P})^2 \times \sum(O_j - \bar{O})^2}}$$	Unitless, $-1 \leq R \leq 1$
2	Normalize mean bias (NMB)	$$\frac{\sum(P_j - O_j)}{\sum O_j} \times 100$$	$-100\% \leq NMB \leq +\infty$
3	Normalize mean error (NME)	$$\frac{\sum|P_j - O_j|}{\sum O_j} \times 100$$	$0\% \leq NME \leq +\infty$
4	Root mean square error (RMSE)	$$\sqrt{\frac{\sum(P_j - O_j)^2}{N}}$$	concentration unit
5	Mean bias (MB)	$$\frac{\sum(P_j - O_j)}{N}$$	concentration unit

Table S2 MOZART species and the corresponding category[*]

Abbreviation	Species	Category
APIN	α-pinene	alkenes
BENZENE	benzene	aromatics
BIGALK	lumped alkanes C>3 (C_5H_{12})	alkanes
BIGENE	lumped alkenes C>3 (C_4H_8)	alkenes
BPIN	beta-pinene ($C_{10}H_{16}$)	alkenes
BZALD	benzaldehyde (C_7H_6O)	OVOCs
C_2H_2	ethyne	ethyne
C_2H_4	ethene	alkenes
C_2H_6	ethane	alkanes
C_3H_6	propene	alkenes
C_3H_8	propane	alkanes
CH_2O	formaldehyde	OVOCs
CH_3CH_2OH	ethanol	OVOCs
CH_3CHO	acetaldehyde	OVOCs
CH_3COCH_3	acetone	OVOCs
CH_3COOH	acetic acid	OVOCs
CH_3OH	methanol	OVOCs
CRESOL	lumped cresols (C_7H_8O)	aromatics
GLYALD	glycolaldehyde	OVOCs
HCOOH	formic acid	OVOCs
ISOP	isoprene (C_5H_8)	alkenes
LIMON	limonene ($C_{10}H_{16}$)	alkenes
MACR	methacrolein	OVOCs

MEK	methyl ethyl ketone (C_4H_8O)	OVOCs
MGLY	methyl glyoxal	OVOCs
MVK	methyl vinyl ketone	OVOCs
PHENOL	phenol (C_6H_5OH)	aromatics
TOLUENE	toluene (C_7H_8)	aromatics
XYLOL	dimethyl phenol ($C_8H_{10}O$)	aromatics

[*] FINN provides emissions of model species for three common VOCs speciations: MOZART, SAPRC99 and GEOS-Chem; the MOZART speciation is used in this study.

Table S3 Emissions from open biomass burning and anthropogenic sources in 2018 (Anthropogenic emissions are based on MEIC 2017 data)

	OBB	OCSB	Transport	Power	Industry	Residential
VOCs emissions (Gg)	1698	799	4229	81	14951	4373
NOx emissions (Gg)	258	81	7973	4220	9328	899
VOCs/NOx ratio	6.58	9.91	0.53	0.02	1.60	4.86

Table S4 Model evaluation statistics of MDA8 ozone concentrations

Region/Season	Observed (μg/m³)	Simulated (μg/m³)	R	MB (μg/m³)	RMSE (μg/m³)	NMB	NME
China	165.1	179.6	0.78	14.5	20.9	9%	11%
North China	191.5	195.9	0.78	4.4	12.6	2%	5%
YRD	165.5	182.9	0.83	17.5	19.7	11%	11%
Sichuan Basin	166.0	202.5	0.99	36.5	37.3	22%	22%
Northeast China	146.6	134.8	0.32	-11.7	19.0	-8%	9%
Guangdong	163.0	184.8	0.64	21.8	25.3	13%	13%
Spring	117.5	126.1	0.31	8.6	17.4	7%	12%
Summer	127.2	138.5	0.90	11.3	16.8	9%	11%
Fall	87.8	97.5	0.65	9.7	18.4	11%	18%
Winter	70.5	74.4	0.59	4.0	14.2	6%	17%

Table S5 Estimated number of ozone exceedances days in different scenarios

Region	City	Number of ozone exceedances days in 2018 (Base Scenario)	Number of ozone exceedances days without OCSB emissions (Scenario 2)	Number of ozone exceedances days before straw burning bans (Scenario 3)
North China	Anyang	78	75	79
	Baoding	100	97	99
	Beijing	67	66	71
	Binzhou	110	109	112
	Cangzhou	93	92	95
	Chengde	52	51	55
	Datong	34	33	35
	Dezhou	100	99	102
	Dongying	94	93	96
	Handan	86	85	89
	Heze	78	76	79
	Hebi	81	81	87
	Hengshui	81	77	82
	Jimo	33	33	36
	Jinan	103	100	103
	Jining	86	85	91
	Jiaonan	34	32	36
	Jiaozhou	22	21	24
	Jiaozuo	88	87	90
	Jincheng	102	102	106
	Jinzhong	64	64	65
	Kaifeng	71	71	75
	Laixi	30	30	31
	Laizhou	23	22	26
	Langfang	73	71	74
	Liaocheng	97	97	99
	Linyi	70	68	75
	Luoyang	76	75	77
	Leihe	60	58	59
	Lvliang	41	40	43

	Nanyang	51	50	54
	Penglai	40	36	43
	Pingdingshan	68	65	70
	Pingdong	43	42	44
	Puyang	75	73	76
	Qinhuangdao	37	34	37
	Qingdao	19	17	23
	Rizhao	29	27	30
	Rongcheng	22	22	22
	Rushan	31	31	33
	Sanmenxia	54	54	57
	Shangqiu	61	58	60
	Jiazhuang	87	83	89
	Shouguang	39	37	42
	Shuozhou	39	38	41
	Taiyuan	74	73	74
	Taian	82	79	82
	Tangshan	75	74	76
	Tianjin	89	85	90
	Weihai	42	41	44
	Weifang	74	72	76
	Wendeng	24	24	25
	Xinzhou	48	48	48
	Xinxiang	93	89	95
	Xinyang	58	57	63
	Xingtai	87	84	88
	Xuchang	59	58	63
	Yantai	34	32	39
	Yangquan	68	67	69
	Yuncheng	88	87	88
	Zaozhuang	80	78	84
	Zhangjiakou	57	57	58
	Zhangqiu	82	80	85
	Changzhi	83	82	85

	Zhaoyuan	18	18	21
	Zhengzhou	78	74	81
	Zhoukou	61	59	65
	Zhumadian	65	65	67
	Zibo	103	100	102
YRD	Anqing	38	37	42
	Bangbu	59	59	62
	Haozhou	59	58	60
	Changshu	31	31	34
	Changzhou	73	73	74
	Chizhou	29	29	31
	Chuzhou	58	56	62
	Fuyang	37	37	41
	Fuyang	6	6	6
	Haimen	27	27	28
	Hangzhou	54	54	57
	Huzhou	71	71	72
	Huaian	54	52	57
	Huaibei	67	65	72
	Huainan	62	61	64
	Jiaxing	55	54	58
	Jiangyin	47	47	49
	Jinhua	37	37	39
	Jintan	77	75	79
	Jurong	47	47	50
	Kunshan	55	55	55
	Lishui	9	9	9
	Liyang	66	65	65
	Linan	21	21	23
	Liuan	47	46	48
	Maanshan	64	61	65
	Nanjing	56	55	62
	Nantong	31	30	33
	Ningbo	25	25	26

	Quzhou	23	23	23
	Shanghai	37	37	39
	Shaoxing	46	46	47
	Suzhou	49	48	52
	Taizhou	14	14	15
	Taicang	45	45	45
	Taizhou	55	55	57
	Tongling	16	15	17
	Wenzhou	10	10	12
	Wuxi	61	59	62
	Wuhu	66	63	68
	Wujiang	48	48	50
	Suqian	57	57	57
	Suzhou	73	72	79
	Xuzhou	63	62	66
	Xuancheng	7	7	8
	Yancheng	45	44	49
	Yangzhou	63	61	63
	Yixing	82	82	84
	Yiwu	14	14	15
	Zhangjiagang	43	43	45
	Zhenjiang	61	60	63
	Zhoushan	13	13	13
	Zhuji	11	11	11
Sichuan Basin	Bazhong	1	1	1
	Chengdong	47	46	47
	Dazhou	15	14	16
	Deyang	29	29	29
	Ganzizhou	2	2	2
	Guangan	19	19	20
	Guangyuan	4	4	4
	Leshan	12	12	12
	Liangshanzhou	5	5	5
	Luzhou	24	23	23

	Meishan	40	40	41
	Mianyang	26	26	28
	Nanchong	23	23	24
	Neijiang	28	26	29
	Panzhihua	7	7	7
	Suining	22	22	23
	Yaan	5	5	5
	Yibin	32	32	35
	Zhongqing	43	43	44
	Ziyang	32	32	33
Northeast China	Anshan	36	35	37
	Baicheng	4	4	4
	Baishan	13	12	16
	Benxi	18	17	20
	Chaoyang	40	39	42
	Dalian	32	30	38
	Daqing	6	6	6
	Dandong	10	10	10
	Fushun	39	39	41
	Fuxin	33	33	36
	Hadongbin	9	9	9
	Hegang	4	4	4
	Heihe	2	2	2
	Huludao	35	35	35
	Jixi	1	1	1
	Jilin	29	28	29
	Jiamusi	5	5	5
	Jinzhou	33	32	33
	Liaoyang	34	33	35
	Liaoyuan	27	26	27
	Mudanjiang	7	7	7
	Panjin	46	45	46
	Qitaihe	23	23	24
	Qiqihadong	4	4	5

	Shenyang	39	37	42
	Shuangyashan	6	6	6
	Siping	36	36	37
	Songyuan	13	12	14
	Suihua	4	4	4
	Tieling	26	25	27
	Tonghua	22	22	22
	Wafangdian	10	9	10
	Yanbianzhou	15	15	16
	Yichun	5	4	5
	Yingkou	66	65	68
	Changchun	14	14	14
PRD and surrounding	Dongwan	42	42	42
	Foshan	48	48	48
	Guangzhou	42	42	42
	Huizhou	17	16	17
	Jiangmen	53	53	53
	Shenzhen	14	14	15
	Zhaoqing	32	32	33
	Zhongshan	38	37	38
	Zhuhai	37	37	37
North China total		4544	4438	4682
YRD total		2447	2414	2550
Sichuan Basin total		479	474	492
Northeast China total		746	728	4777
PRD and surrounding total		323	321	325
Five regions total		8539	8375	8826

35

Table S6 Estimated number of premature mortality in different scenarios

Region	Province	Base Scenario			Scenario 2			Scenario 3		
		RD	CVD	Total	RD	CVD	Total	RD	CVD	Total
Northeast China	Liaoning	4810 (3380-6100)	2970 (1020-4810)	7780 (4400-10910)	4760 (3350-6050)	2940 (1010-4760)	7700 (4360-10800)	4850 (3410-6140)	2990 (1030-4840)	7840 (4440-10980)
	Heilongjiang	2540 (1770-3250)	1530 (520-2500)	4070 (2290-5750)	2500 (1740-3210)	1510 (520-2460)	4010 (2260-5670)	2530 (1760-3230)	1530 (520-2480)	4060 (2280-5710)
	Jilin	2100 (1470-2670)	1280 (440-2080)	3380 (1910-4750)	2080 (1460-2650)	1270 (430-2060)	3350 (1890-4720)	2110 (1470-2680)	1290 (440-2090)	3400 (1910-4770)
North China	Hebei	10560 (7490-13280)	6660 (2300-10740)	17220 (9790-24020)	10430 (7390-13120)	6570 (2260-10590)	17000 (9650-23710)	10720 (7610-13470)	6770 (2340-10910)	17490 (9950-24380)
	Shandong	14680 (10430-18420)	9300 (3210-14970)	23980 (13640-33390)	1390 (990-1750)	880 (300-1410)	2270 (1290-3170)	14890 (10590-18670)	9450 (3260-15210)	24340 (13850-33880)
	Tianjin	1410 (1000-1780)	890 (310-1430)	2300 (1310-3210)	1940 (1380-2440)	1230 (420-1980)	3170 (1800-4420)	1430 (1020-1800)	900 (310-1460)	2330 (1330-3260)
	Beijing	1970 (1400-2470)	1250 (430-2010)	3220 (1830-4480)	5360 (3840-6680)	3450 (1200-5540)	8810 (5040-12220)	1990 (1420-2500)	1260 (440-2030)	3250 (1860-4530)
	Henan	13440 (9600-16780)	8610 (2980-13830)	22050 (12580-30610)	14550 (10340-18260)	9200 (3180-14830)	23750 (13520-33090)	13600 (9720-16980)	8730 (3030-14020)	22330 (12750-31000)
	Shanxi	5380 (3850-6710)	3470 (1200-5560)	8850 (5050-12270)	13330 (9520-16650)	8540 (2960-13710)	21870 (12480-30370)	5420 (3880-6750)	3500 (1210-5610)	8920 (5090-12360)
YRD	Shanghai	2670 (1890-3360)	1680 (580-2710)	4350 (2470-6070)	11580 (8230-14540)	7330 (2530-11810)	18910 (10760-26350)	2690 (1910-3380)	1690 (580-2730)	4380 (2490-6110)
	Anhui	9390 (6700-11740)	6000 (2070-9640)	15390 (8770-21380)	7350 (5220-9220)	4660 (1610-7500)	12010 (6830-16720)	9470 (6760-11840)	6060 (2100-9740)	15530 (8860-21580)
	Jiangsu	11650 (8280-14620)	7380(2550-11890)	19030 (10830-26510)	2660 (1890-3350)	1680 (580-2700)	4340 (2470-6050)	11750 (8360-14740)	7450 (2570-12000)	19200 (10930-26740)
	Zhejiang	7370 (5240-9240)	4670 (1610-7520)	12040 (6850-16760)	9330 (6650-11670)	5950 (2060-9570)	15280 (8710-21240)	7400 (5260-9290)	4690 (1620-7560)	12090 (6880-16850)
Sichuan Basin	Sichuan	14400 (10300-17970)	9250 (3210-14850)	23650 (13510-32820)	14360 (10270-17920)	9230 (3200-14810)	23590 (13470-32740)	14420 (10310-17990)	9270 (3210-14880)	23690 (13520-32870)
	Chongqing	4250 (3010-5350)	2660 (920-4300)	6910 (3930-9650)	4240 (3000-5340)	2660 (910-4290)	6900 (3910-9630)	4260 (3010-5360)	2670 (920-4310)	6930 (3930-9670)
PRD and surrounding	Guangdong	10690 (7580-13450)	6730 (2320-10860)	17420 (9900-24310)	10670 (7570-13430)	6720 (2320-10840)	17390 (9890-24270)	10710 (7590-13470)	6740 (2330-10880)	17450 (9920-24350)
	Tibet	510	330	840	8110	5190	13300	510	330	840

		Col1	Col2	Col3	Col4	Col5	Col6	Col7	Col8	Col9
Other		(370-630)	(110-530)	(480-1160)	(5790-10130)	(1800-8340)	(7590-18470)	(370-630)	(110-530)	(480-1160)
	Hunan	9200 (6530-11550)	5820 (2010-9370)	15020 (8540-20920)	9170 (6520-11520)	5800 (2000-9340)	14970 (8520-20860)	9240 (6560-11590)	5840 (2020-9410)	15080 (8580-21000)
	Jiangxi	5460 (3870-6860)	3440 (1190-5540)	8900 (5060-12400)	4460 (3160-5600)	2810 (970-4530)	7270 (4130-10130)	5480 (3880-6880)	3450 (1190-5560)	8930 (5070-12440)
	Hainan	650 (460-830)	400 (140-650)	1050 (600-1480)	5440 (3860-6840)	3430 (1180-5530)	8870 (5040-12370)	660 (460-830)	400 (140-650)	1060 (600-1480)
	Guangxi	5350 (3780-6770)	3330 (1150-5390)	8680 (4930-12160)	650 (460-830)	400 (140-650)	1050 (600-1480)	5360 (3780-6780)	3340 (1150-5400)	8700 (4930-12180)
	Inner Mongolia	2460 (1740-3090)	1540 (530-2480)	4000 (2270-5570)	5350 (3770-6760)	3330 (1140-5380)	8680 (4910-12130)	2460 (1740-3100)	1540 (530-2490)	4000 (2270-5590)
	Hubei	8140 (5820-10170)	5220 (1810-8380)	13360 (7630-18550)	510 (370-630)	330 (110-530)	840 (480-1160)	8190 (5850-10230)	5250 (1820-8430)	13440 (7670-18660)
	Yunnan	5520 (3880-6990)	3410 (1170-5520)	8930 (5050-12510)	5510 (3880-6990)	3400 (1170-5520)	8910 (5050-12510)	5520 (3880-7000)	3410 (1170-5530)	8930 (5050-12530)
	Fujian	4460 (3170-5610)	2820 (970-4540)	7280 (4140-10150)	4060 (2860-5140)	2510 (860-4070)	6570 (3720-9210)	4470 (3170-5620)	2820 (970-4550)	7290 (4140-10170)
	Guizhou	4070 (2860-5150)	2520 (860-4080)	6590 (3720-9230)	2540 (1810-3170)	1620 (560-2600)	4160 (2370-5780)	4080 (2870-5160)	2520 (870-4090)	6600 (3740-9250)
	Xinjiang	2540 (1810-3170)	1620 (560-2600)	4160 (2370-5770)	2450 (1730-3090)	1530 (530-2480)	3980 (2260-5560)	2540 (1810-3170)	1620 (560-2600)	4160 (2370-5770)
	Qinghai	890 (640-1110)	570 (200-920)	1460 (840-2030)	890 (640-1110)	570 (200-920)	1460 (840-2030)	890 (640-1110)	580 (200-920)	1470 (840-2030)
	Gansu	3660 (2610-4570)	2340 (810-3760)	6000 (3420-8330)	3650 (2610-4560)	2340 (810-3760)	5990 (3420-8320)	3660 (2620-4570)	2350 (810-3770)	6010 (3430-8340)
	Ningxia	840 (600-1050)	540 (190-860)	1380 (790-1910)	840 (600-1050)	530 (180-860)	1370 (780-1910)	840 (600-1060)	540 (190-860)	1380 (790-1920)
	Shaanxi	5330 (3810-6660)	3410 (1180-5480)	8740 (4990-12140)	5310 (3790-6640)	3400 (1180-5460)	8710 (4970-12100)	5350 (3820-6680)	3430 (1190-5510)	8780 (5010-12190)
Total		176390 (125340-221400)	111640 (38550-179800)	288030 (163890-401200)	175470 (124690-220340)	111010 (38320-178830)	286480 (163010-399190)	177490 (126130-222700)	112410 (38830-181050)	289900 (164960-403750)

Figure S1 NO*x* emissions from OCSB by month and region in 2018 (unit: Gg)

Changes in number of ozone exceedances days
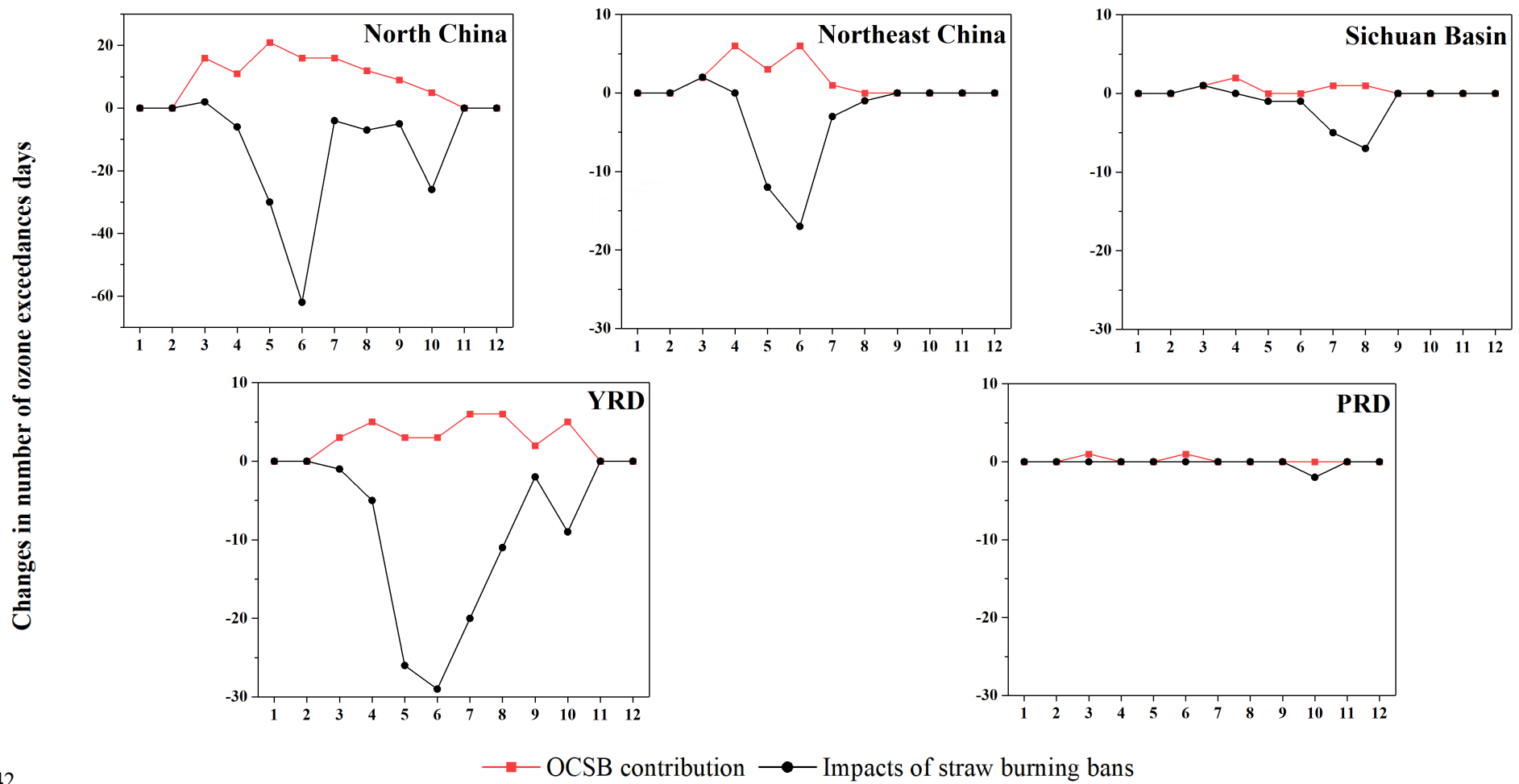
Legend: OCSB contribution — Impacts of straw burning bans

42

43   **Figure S2 The number of days of MDA8 O$_3$ exceeding the standard caused by OCSB and straw burning bans in 2018**
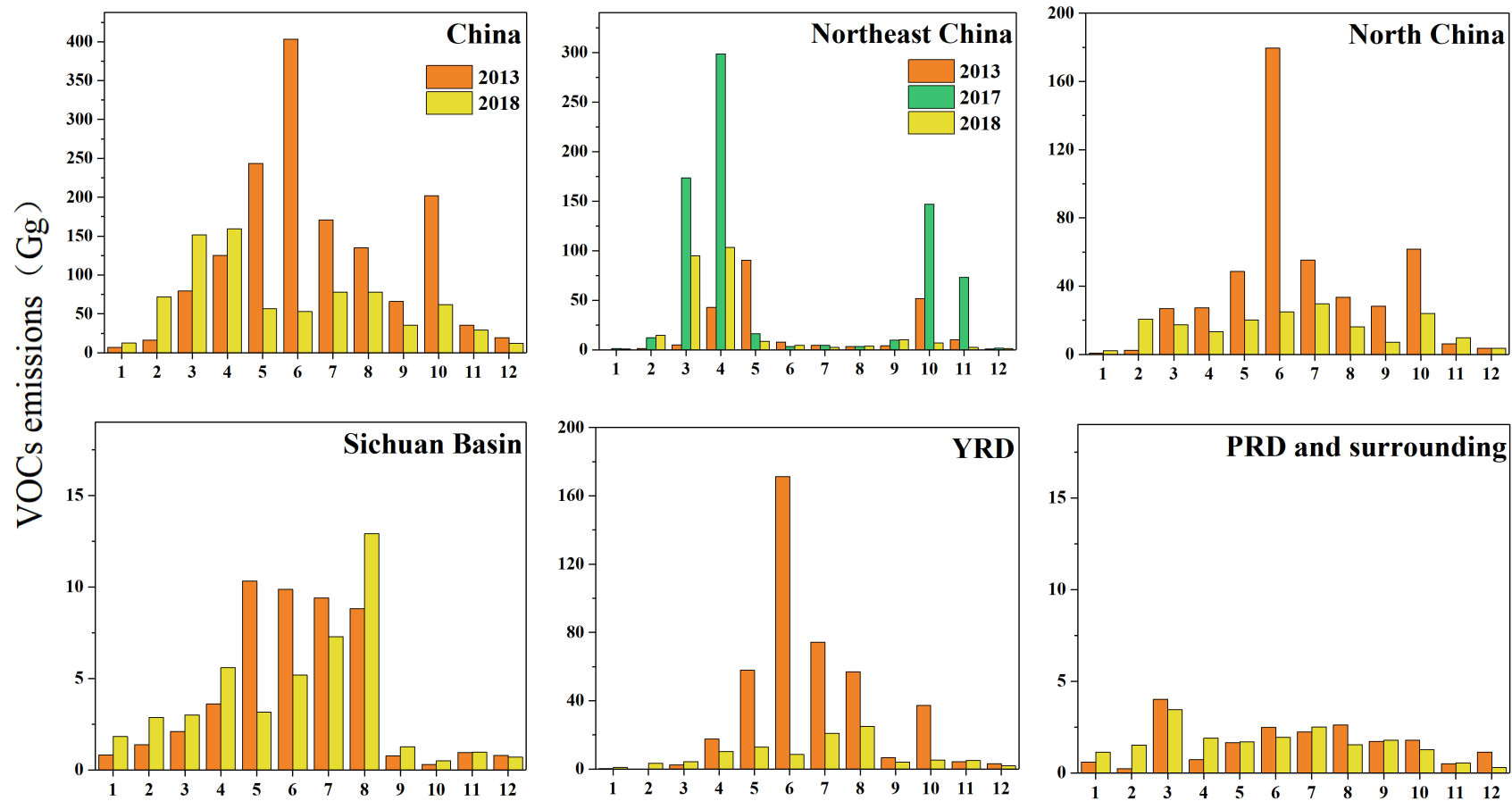
Figure S3 Monthly VOCs emissions from OCSB in 2013 and 2018

47
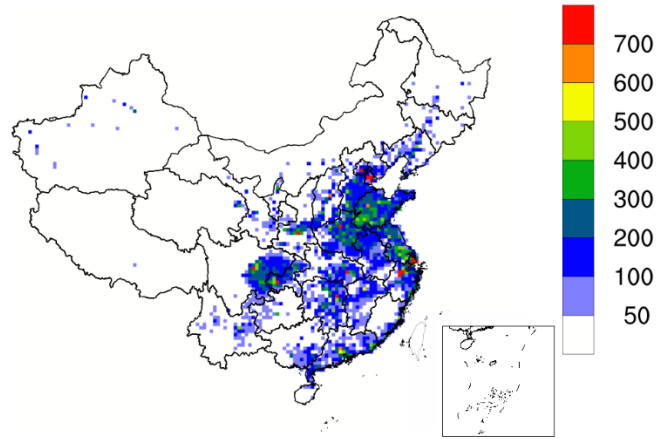
Figure S4 Spatial distribution of premature mortality associated with ozone exposure in 2018 (No data for Taiwan, Hong Kong and Macau) Unit: person/grid